A Theoretical Study of the Low-Lying Excited States of *trans*- and *cis*-Urocanic Acid

Christopher S. Page, Manuela Merchán,* and Luis Serrano-Andrés

Departamento de Química Física, Universitat de València, Dr. Moliner 50, Burjassot, E-46100 València, Spain

Massimo Olivucci*

Istituto di Chimica Organica, Università degli Studi di Siena, Via Aldo Moro, I-53100 Siena, Italy

Received: May 19, 1999; In Final Form: September 7, 1999

A multiconfigurational second-order perturbation theory (CASPT2) study of the lowest lying states in the gas-phase electronic spectra of *trans*- and *cis*-urocanic acid is presented. Geometries of both isomers have been optimized at the MP2/6-31G(d) and π-CASSCF/ANO-L(4s3p1d,2s) levels of theory. The geometries are found to differ considerably between the two levels. The vertical and 0−0 excitation spectra were calculated for each isomer. Both singlet and triplet states are described for each, including the lowest lying $\pi\pi^*$ excitations and the $n_O\pi^*$ excitations. Remarkably, in the trans spectrum, it is found that the $n_O\pi^*$ state has a higher vertical excitation energy than the lowest $\pi\pi^*$ (5.12 vs 4.93 eV), but a lower band origin (4.10 vs 4.66 eV). Thus, the $\pi\pi^*$ and $n_O\pi^*$ surfaces cross at a coordinate between that of the ground-state structure and the equilibrium excited state structure. The trans vertical spectrum consists of three intense ($\pi\pi^*$) electronic transitions at 4.93, 5.40, and 6.00 eV, whereas the cis spectrum is dominated by a single intense transition at 4.15 eV and a weaker one at 5.85 eV. The wave functions of the excitations typically show a multiconfigurational character, with the weighting of doubly excited configurations exceeding 20% in a number of instances. The lowest lying Rydberg states (π3s) were found at 5.47 and 5.67 eV for the trans and cis isomers, respectively.

1. Introduction

Urocanic acid (4-imidazoleacrylic acid; Figure 1) is a metabolic product of histidine, formed by the enzyme histidase. Occurring naturally in the E (trans) form, it acts as a substrate for the enzyme urocanase. In the mammalian epidermis, where urocanase is absent, urocanic acid is found to accumulate, accounting for 0.7% of the dry weight of the human stratum corneum.[1]

Urocanic acid is a major UV chromophore, absorbing strongly in the UV-B region (300−280 nm; 4.13−4.43 eV). Irradiation at these wavelengths has been shown to bring about lesions in DNA at neighboring pyrimidines that can ultimately lead to skin cancer.[2] Indeed, the remarkable similarity between the photocarcinogenic action spectrum and the absorption spectrum for *trans*-urocanic acid in this region[3] has led to its being proclaimed a "natural sunblock" and, for many years, to its inclusion in artificial sunlotions. Ironically, its use as such was discontinued in the early 1990s, following the discovery that the cis isomer, itself a UV-B photoproduct, has a selective immunosuppressive role that may be attributed to its being an analogue of the immunoregulator histamine.[4] The link between immunosuppression and tumour growth is well established and the photoisomerization of urocanic acid has thus been implicated as a pertinent process in photocarcinogenesis,[5] although the mechanism is unclear. Other effects of this suppression of immune responses include a down regulation of contact and delayed-type hypersensitivity,[6] and an alteration in the morphology and function of the epidermal Langerhans cells.[7]

In terms of its photochemistry, *trans*-urocanic acid has proved to be a puzzling molecule. The efficiency of its isomerization is wavelength dependent. The process shows a maximum efficiency at low excitation energies (~4.0 eV), but this efficiency is very much reduced at the higher excitation energies (~4.7 eV) where peak absorption is observed.[8,9]

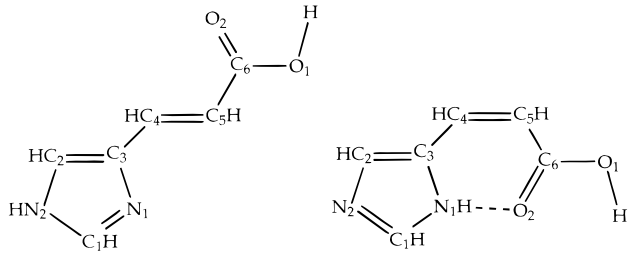

Figure 1. Schematic representations of *trans*- and *cis*-urocanic acid. Note that the most stable tautomers differ in the protonation of the imidazole ring.

Hanson and Simon have recently provided evidence that the wavelength dependence of urocanic acid isomerization in solution is a consequence of the presence of multiple electronic states with overlapping absorption transitions that are not easily distinguished.[9,10] In particular, they conclude that it is the excitation to either the singlet $n\pi^*$ or singlet $\pi\pi^*$ states that gives rise to the trans → cis isomerization or internal conversion, respectively. This view is concurrent with the behavior observed in the urocanic acid analogue, cinnamic acid:[11,12] in this case, the absorption spectrum is completely dominated by a $\pi\pi^*$ transition from the phenyl ring, with a weak $n\pi^*$ transition forming the red tail (<4.1 eV) of the profile.

In this paper, results are presented of a computational investigation of the *trans*- and *cis*-urocanic acid vertical and 0−0 excitation spectra. These data will provide a basis for the comprehension of the electronic structure of the molecule. The

10.1021/jp991657d CCC: $18.00
Published on Web 11/11/1999

TABLE 1: CASSCF Wave Functions Used To Compute the Valence and Rydberg Transitions of *trans*- and *cis*-Urocanic Acid[a]

wave function[b]	state	no. conf.[c]	N_{states}[d]
CASSCF (I: 20 0; A: 0 10) (12)	$1-5^1A'(\pi\pi^*)$	13 860	5
	$1-2^3A'(\pi\pi^*)$	20 790	3
CASSCF (I: 19 0; A: 1 10) (14)	$1-2^1A''(\pi\pi^*)$	13 860	1
	$1-2^3A''(\pi\pi^*)$	23 100	1
CASSCF (I: 20 0; A: 1 10) (12)	$^1A''(\pi 3s)$	27 720	1
CASSCF (I: 20 0; A: 0 10) (11)	$1^2A''$	27 720	1
CASSCF (I: 19 0; A: 1 10) (13)	$1-2^2A'$	34 650	1

[a] Core orbitals have been kept frozen at the scf level (F: 10 0). [b] Within parentheses the number of frozen (F), inactive (I), and active (A) orbitals of symmetry a′−a″ of the point group C_s. [c] Number of configurations in the CASSCF wave function. [d] States included in the average CASSCF wave function.

present study concentrates on the photophysics and photochemistry of the neutral form of the molecule in its ground or electronically excited state equilibrium structures. In a following paper, the emphasis will be on changes in electronic structure due to deprotonation of the neutral form (the pK_a of the carboxylic oxygen is 3.5[13]), which gives rise to the "reactive" carboxylate anion observed in vivo, and further to structural and electronic changes occurring during isomerization.

To date, the gas-phase spectroscopy of urocanic acid has not been reported, and it is hoped that the findings presented herein will provide both an impetus and an interpretation for such an experiment.

2. Methods and Computational Details

Geometry optimizations for the ground state and low-lying excited states were carried out at the CASSCF level using the generally contracted basis sets of the atomic natural orbital (ANO-L) type, obtained from the C,N,O(14s9p4d)/H(8s) primitive sets.[14] The contraction scheme C,N,O[4s3p1d]/H[2s] was used in the present study, comprising a total of 192 basis functions. The active space for the ground state was chosen to include all π-valence electrons, as described below and defined in Table 1; similarly, excited state geometry optimizations used the same active spaces as were defined for vertical excitations. For comparative purposes, the geometries of ground-state *trans*- and *cis*-urocanic acid were also optimized at the Hartree−Fock (HF) and MP2 levels employing the 6-31G(d) basis set. Full geometry optimizations were performed assuming planar structures with C_s symmetry (29 degrees of freedom). The CASSCF-optimized geometries for the ground states were employed in the calculation of the vertical excitation energies of the two isomers.

The low-lying states were computed using multiconfigurational second-order perturbation theory as defined by the CASPT2 protocol.[15,16] The CASSCF procedure[17] determined the multiconfigurational single-reference function employed in the perturbational treatment. The molecular orbitals for the excited states were obtained from state average CASSCF calculations, where the averaging included all states of interest of a given symmetry. The number of states included in the state average CASSCF calculations, the number of configurations in the CASSCF wave function, details of the active spaces used, and the type of states computed are given in Table 1.

The closed-shell HF description of the $C_6H_6N_2O_2$ system has (30−6) occupied orbitals of symmetry (a′−a″). The π orbitals belong to the a″ irreducible representation of the point group C_s. For the singlet and triplet states of A′ symmetry, the π-valence active space (0−10) has been employed (10π active orbitals with 12π active electrons), for what will henceforth be denoted as the π-CASSCF wave function. For the $\pi\pi^*$ states, the lone pairs of the heteroatoms behave as inactive orbitals: it is found that the occupation numbers are close to 2.0 when they are treated as active. The same active space (11 active electrons) was used to determine the vertical ionization potential to the $1^2A''(\pi$-hole) state. For the $^{1,3}A''(n\pi^*)$ states the active space also included either the lone pair on the oxygen atom or on the nitrogen atom as appropriate (i.e., 1−10) with 14 active electrons). The same active space (with 13 active electrons) was employed to compute the vertical ionization potentials to the $1^2A'(n$-hole) states. In order to predict the lowest Rydberg state, the vertical ionization potentials were computed at the π-CASSCF/CASPT2 level. As can be seen in Table 2, the lowest ionization potential involves a π-hole. Accordingly, the $^1A''(\pi \rightarrow 3s)$ was computed to be the lowest singlet Rydberg state.

TABLE 2: CASSCF and CASPT2 Calculated Vertical Ionization Potentials (eV) for *trans*- and *cis*-Urocanic Acid[a]

state	CASSCF	CASPT2
	trans-Urocanic Acid	
$1^2A''$ (π-hole)	7.80 (7.73)	8.33 (8.29)
$1^2A'$ (n_N-hole)	9.26 (9.16)	10.16 (10.15)
$2^2A'$ (n_O-hole)	9.10 (8.96)	10.18 (10.13)
	cis-Urocanic Acid	
$1^2A''$ (π-hole)	7.03 (7.02)	8.33 (8.33)
$1^2A'$ (n_N-hole)	8.96 (8.96)	9.92 (9.92)
$2^2A'$ (n_O-hole)	9.88 (9.87)	10.88 (10.88)

[a] Values are given for both the CASSCF and MP2 optimized geometries, the latter appearing within parentheses.

The inclusion of diffuse functions is required to treat the 3*s* Rydberg state adequately. Adopting the procedure described in detail elsewhere,[18] custom 1s1p1d sets of Rydberg functions (contracted from a set of 8s8p8d primitive functions) were built for *trans*- and *cis*-urocanic acid. The valence basis set of ANO type C,N,O[4s3p1d]/H[2s] was supplemented with these Rydberg functions, which were placed in the average charge centroid of the $1^2A''$ (π-hole) state of the cation for the corresponding isomer. The π-valence active space was enlarged to (1−12), with an additional orbital of a′ symmetry, to describe the $^1A''$-($\pi \rightarrow$ 3s) Rydberg state (12 active electrons).

The relative energy of each excited state is referred to a ground-state energy computed with the same active space. The carbon, nitrogen, and oxygen 1s electrons were kept frozen in the form determined by the ground-state HF wave function. The core electrons were inactive in the π-CASSCF geometry optimization process. All electrons except the core electrons were correlated at the CASPT2 level.

The transition dipole moments were computed by means of the CASSCF state interaction (CASSI) method.[19,20] In calculating the oscillator strength, the vertical excitation energy computed at the CASPT2 level was employed.[18,21,22]

The CASSCF/CASPT2 and CASSI calculations were performed using the MOLCAS 4.1 quantum chemistry software.[23] The computations employing the 6-31G(d) basis set at the HF and MP2 levels were carried out using the Gaussian 94 suite.[24] Default convergence criteria implemented in the respective programs were used in all parameter optimizations.

All calculations were carried out on the Silicon Graphics Origin 2000 server of the University of Valencia.

3. Results and Discussion

3.1. Geometries. The atom numbering scheme used throughout this study of urocanic acid is defined in Figure 1.

TABLE 3: Equilibrium Geometries (Bond Lengths in Å; Angles in deg) for Ground-State *trans*- and *cis*-Urocanic Acid Optimized at the MP2 and CASSCF Levels (C_s Symmetry)

	trans		cis	
bond/angle	MP2 (HF)[a]	CASSCF (HF)[b]	MP2 (HF)[a]	CASSCF (HF)[b]
N_1-C_1	1.321 (1.285)	1.294 (1.283)	1.356 (1.333)	1.352 (1.334)
C_1-N_2	1.368 (1.353)	1.363 (1.353)	1.335 (1.302)	1.306 (1.301)
N_2-C_2	1.371 (1.365)	1.374 (1.367)	1.362 (1.353)	1.366 (1.355)
C_2-C_3	1.387 (1.357)	1.366 (1.355)	1.398 (1.368)	1.376 (1.365)
C_3-N_1	1.384 (1.376)	1.384 (1.377)	1.377 (1.375)	1.374 (1.374)
C_3-C_4	1.447 (1.456)	1.453 (1.452)	1.435 (1.442)	1.443 (1.437)
C_4-C_5	1.348 (1.327)	1.341 (1.324)	1.359 (1.339)	1.351 (1.337)
C_5-C_6	1.470 (1.474)	1.475 (1.473)	1.463 (1.467)	1.471 (1.465)
C_6-O_1	1.364 (1.332)	1.329 (1.330)	1.358 (1.328)	1.324 (1.325)
C_6-O_2	1.224 (1.193)	1.188 (1.189)	1.232 (1.201)	1.193 (1.196)
C_1-H	1.083 (1.071)	1.072 (1.073)	1.082 (1.071)	1.072 (1.073)
C_2-H	1.082 (1.068)	1.070 (1.070)	1.083 (1.071)	1.072 (1.072)
C_4-H	1.089 (1.076)	1.078 (1.078)	1.090 (1.077)	1.079 (1.080)
C_5-H	1.085 (1.072)	1.075 (1.074)	1.085 (1.073)	1.076 (1.075)
$N_{1/2}-H$	1.013 (0.994)	0.997 (0.997)	1.022 (0.998)	0.998 (1.000)
O_1-H	0.980 (0.951)	0.959 (0.959)	0.980 (0.951)	0.959 (0.956)
$O_2\cdots H(N_1)$			1.842 (1.929)	1.974 (1.947)
$N_1-C_1-N_2$	111.73 (112.17)	112.16 (112.18)	112.23 (112.81)	112.45 (112.74)
$C_1-N_2-C_2$	107.58 (106.82)	106.66 (106.72)	104.49 (104.82)	104.95 (104.83)
$N_2-C_2-C_3$	105.27 (105.57)	105.74 (105.64)	111.37 (111.02)	110.86 (110.99)
$C_2-C_3-N_1$	110.20 (109.78)	109.69 (109.75)	104.24 (104.35)	104.61 (104.41)
$C_3-N_1-C_1$	105.22 (105.65)	105.75 (105.71)	107.67 (106.99)	107.13 (107.03)
$C_2-C_3-C_4$	127.28 (126.88)	126.97 (126.50)	127.94 (126.99)	126.80 (126.85)
$C_3-C_4-C_5$	123.95 (124.92)	124.93 (125.33)	132.99 (133.91)	133.89 (134.17)
$C_4-C_5-C_6$	119.51 (119.77)	120.47 (120.11)	127.65 (127.39)	128.19 (127.66)
$C_5-C_6-O_1$	111.24 (112.03)	111.88 (111.89)	110.48 (111.31)	111.17 (111.37)
$C_5-C_6-O_2$	126.56 (126.18)	126.01 (126.21)	128.89 (127.98)	127.54 (127.76)
N_1-C_1-H	125.87 (125.72)	125.68 (125.78)	122.48 (122.26)	122.15 (122.16)
$C_1-N_{1/2}-H$	126.41 (126.57)	126.47 (126.51)	129.94 (128.87)	128.30 (128.73)
N_2-C_2-H	122.52 (122.57)	122.51 (122.62)	121.51 (121.64)	121.70 (121.75)
C_3-C_4-H	117.92 (116.67)	116.56 (116.18)	112.07 (111.29)	111.49 (111.08)
C_4-C_5-H	121.53 (122.19)	121.86 (122.03)	117.91 (118.18)	117.68 (117.88)
C_6-O_1-H	105.14 (107.81)	107.53 (107.45)	105.60 (108.16)	107.87 (107.72)
$C_6-O_2\cdots H(N_1)$			117.75 (120.38)	120.26 (120.49)
$O_2\cdots H-N_1$			142.49 (137.55)	136.96 (136.95)

[a] 6-31G(d) basis set; optimized to default tolerances using Gaussian 94.[24] [b] ANO-L C,N,O[4s3p1d]/H[2s] basis set; optimized to default tolerances using MOLCAS 4.1.[23]

With respect to the protonation sites on the imidazole ring, geometry optimizations at the MP2/6-31G(d) level showed that the trans conformer given in Figure 1, protonated at N_2, was more stable than its N_1 protonated tautomer by some 1.24 kcal mol^{-1}. Conversely, the cis conformer shown in Figure 1, protonated at N_1, was more stable than its N_2 protonated tautomer by 13.57 kcal mol^{-1}, due to the intramolecular N—H···O═C hydrogen bond. The cis isomer containing the hydrogen bond is 3.12 kcal mol^{-1} lower in energy than the N_2 protonated trans isomer. It is expected that, in aqueous solution, competing hydrogen-bonding interactions with the solvent will bring about a change in the cis situation and that the N_2 protonated form of both isomers will be the more stable.

Only the most stable tautomers of urocanic acid, as depicted in Figure 1, shall be considered further here.

The optimized geometric data for the ground states of *trans*- and *cis*-urocanic acid are given in Table 3; corresponding data for the lowest-lying $\pi\pi^*$ and $n\pi^*$ singlet and triplet excited states are given in Table 4. All optimizations were constrained to C_s symmetry, so dihedral angles have been omitted from the tables; these may simply be inferred from Figure 1.

Since analytical gradients are not yet available at the CASPT2 level, it was not possible to include a correction for dynamical correlation in the excited state geometry optimizations. The applicability of a purely CASSCF wave function to these geometric studies was tested on the ground state with additional optimizations at the Hartree−Fock (HF) and MP2 levels. Table 3 presents data for all three treatments.

It can be seen that the HF geometries obtained with MOLCAS and the ANO-L basis set are essentially identical to those obtained using Gaussian 94 and 6-31G(d). Differences in software and basis set used can therefore be ruled out as a source of any discrepancy between the correlated levels.

In general, covalent double bonds in both systems lengthen when electron correlation terms are included in the calculation. However, in the regions of high delocalization, the differences in the extent of this lengthening between the MP2 and CASSCF methods are quite remarkable, with deviations as large as 0.03 Å occurring within the imidazole ring, and similarly within the carboxylic acid group. It is, however, difficult to say at present which of the two is "more correct". The MP2 geometry may be regarded as showing more conjugation than that obtained with CASSCF. This feature is connected with the previously observed effect that methodologies—such as Møller−Plesset perturbation theory and DFT—that are based on single-reference wave functions, but that include large dynamic correlation corrections, usually overestimate π-conjugation.[25] This effect can be clearly seen in Table 3 by comparing the ground-state bond lengths of the double and single bonds. In the case of MP2, they are much closer, with rms deviations from the mean (non-[C,O,N]−H) bond lengths of 0.202 Å (trans) and 0.186 Å (cis), compared with 0.241 Å (trans) and 0.227 Å (cis) at the

TABLE 4: Equilibrium Geometries (Bond Lengths in Å; Angles in deg) for Excited-State *trans*- and *cis*-Urocanic Acid Optimized at the CASSCF Level (C_s Symmetry)

	trans				cis			
bond/angle	$2^1A'$	$1^1A''$	$1^3A'$	$1^3A''$	$2^1A'$	$1^1A''$	$1^3A'$	$1^3A''$
N_1-C_1	1.338	1.292	1.286	1.292	1.317	1.359	1.370	1.359
C_1-N_2	1.375	1.362	1.369	1.362	1.364	1.301	1.312	1.301
N_2-C_2	1.389	1.381	1.380	1.381	1.322	1.367	1.346	1.367
C_2-C_3	1.509	1.383	1.417	1.382	1.434	1.391	1.452	1.388
C_3-N_1	1.357	1.394	1.407	1.394	1.386	1.382	1.377	1.381
C_3-C_4	1.385	1.417	1.377	1.419	1.412	1.416	1.365	1.420
C_4-C_5	1.452	1.443	1.487	1.439	1.440	1.430	1.472	1.421
C_5-C_6	1.448	1.321	1.449	1.323	1.417	1.346	1.446	1.351
C_6-O_1	1.340	1.337	1.332	1.337	1.350	1.343	1.337	1.344
C_6-O_2	1.202	1.352	1.193	1.349	1.248	1.359	1.205	1.354
C_1-H	1.070	1.073	1.073	1.073	1.071	1.067	1.072	1.072
C_2-H	1.066	1.069	1.068	1.069	1.072	1.065	1.072	1.071
C_4-H	1.074	1.076	1.074	1.077	1.075	1.077	1.076	1.076
C_5-H	1.072	1.074	1.072	1.074	1.076	1.075	1.078	1.078
$N_{1/2}-H$	0.995	0.996	0.996	0.996	1.039	1.031	0.993	0.994
O_1-H	0.958	0.955	0.958	0.955	0.956	0.956	0.955	0.955
$O_2\cdots H(N_1)$					1.589	2.113	2.012	2.125
$N_1-C_1-N_2$	112.77	112.62	113.46	112.60	112.37	112.38	112.59	112.36
$C_1-N_2-C_2$	107.99	106.70	106.89	106.69	105.37	105.17	105.80	105.15
$N_2-C_2-C_3$	103.57	105.72	105.37	105.73	110.57	111.28	111.02	111.28
$C_2-C_3-N_1$	108.20	108.91	108.11	108.93	103.62	103.50	102.36	103.59
$C_3-N_1-C_1$	107.46	106.05	106.17	106.05	108.07	107.67	108.24	107.62
$C_2-C_3-C_4$	127.36	128.16	128.47	128.21	132.06	126.78	126.85	126.67
$C_3-C_4-C_5$	121.43	123.12	122.27	123.09	127.53	133.45	131.41	133.57
$C_4-C_5-C_6$	121.28	123.95	120.50	124.06	130.37	132.63	129.49	132.80
$C_5-C_6-O_1$	113.27	124.71	112.83	124.62	113.18	122.97	112.02	122.67
$C_5-C_6-O_2$	124.97	124.54	125.06	124.46	129.42	126.03	127.18	126.00
N_1-C_1-H	124.38	125.42	125.10	125.43	123.49	125.70	122.23	125.70
$C_1-N_{1/2}-H$	125.60	126.44	126.29	126.45	131.55	124.79	127.45	124.82
N_2-C_2-H	124.49	122.53	123.12	122.51	122.63	121.79	122.52	121.79
C_3-C_4-H	119.76	117.43	120.07	117.36	115.57	112.75	114.88	112.53
C_4-C_5-H	120.19	119.44	120.26	119.47	115.18	115.21	115.96	115.33
C_6-O_1-H	107.71	111.20	107.36	111.22	106.50	111.29	107.88	111.33
$C_6-O_2\cdots H(N_1)$					112.89	117.40	119.04	117.33
$O_2\cdots H-N_1$					155.09	133.23	137.79	133.00

CASSCF level. However, CASSCF-optimized geometries have been successfully tested against experimental data for protonated Schiff bases by reproducing the vibrational structure of the resonance Raman (RR) spectra.[26] For this reason, it is believed that the CASSCF geometries are the closer to the actual gas-phase structure. Nevertheless, vertical excitation energies have been computed for both geometries for the sake of comparison.

The geometries of the intramolecular hydrogen bond in the cis conformers are included in the tables. Here, the importance of dynamical correlation becomes very significant, the contact being some 0.13 Å shorter in the MP2 geometry as compared to the CASSCF ground state, with a consequential deformation of the local covalent bond angles. It can further be seen that whereas there is a contraction of the hydrogen bond in the $2^1A'$ excited state (the N—H···O angle tending toward linearity), there is a marked relaxation in the $1^3A'$, $1^1A''$, and $1^3A''$ geometries.

Comparison of the excited state geometries to their CASSCF ground state counterparts reveals some interesting features, which are generally common to both isomers. In terms of bond distances, it can be seen that in all cases, $C_4=C_5$ is lengthened by 0.1 Å or more, the lengthening being most pronounced in the $1^3A'$ geometries. The $2^1A'$ states of both systems also show notable lengthening of the $C_1=N$ and $C_2=C_3$ bonds, but whereas the trans has a shorter C_3-C_4, the cis shows a contraction of C_5-C_6. The A″ states all show similar behavior, with contraction between C_5-C_6 and lengthening between $C_6=O_2$ as well as a ca. 10 deg widening of the $C_5-C_6-O_1$ angle, as would be expected with an excitation of the oxygen lone pair.

3.2. Vertical Spectra of Urocanic Acid. Compiled in Table 5 are the computed vertical excitation energies, oscillator strengths, dipole moments, and transition dipole moment directions of the trans and cis isomers of urocanic acid, in their respective ground-state equilibrium geometries, at the CASSCF and CASPT2 levels of theory. Table 6 lists the contributions to the CASSCF wave functions of the computed states.

Comparing MP2 with CASSCF geometries, it can be seen that with the trans isomer, the singlet vertical excitation energies are red-shifted by as much 0.42 eV at the CASSCF level and 0.31 eV with the CASPT2 correction. Triplet $n\pi^*$ excitations show huge differences at the CASSCF level (1.01 eV, 0.60 eV), but this disparity largely disappears with the inclusion of dynamical correlation. Qualitatively, the vertical spectrum is unchanged: the ordering of the states and the nature of the CASSCF wave function are essentially identical. Intriguingly, the cis isomer yields a quantitatively identical spectrum for both CASSCF and MP2 geometries. This is in spite of a rms difference in bond lengths of 0.075 Å.

With these points in mind, and in view of the remarks made in section 3.1 on the overestimation of conjugation in the MP2 structures, the following discussion shall be restricted to the CASSCF geometries.

The vertical absorption spectrum of *trans*-urocanic acid is dominated up to 6.9 eV by three prominent electronic transitions computed as $\pi\pi^*$ transitions, at 4.93 eV (oscillator strength 0.120), 5.40 eV (0.343), and 6.00 eV (0.324). An analysis of the CASSCF wave function for the states (Table 6) reveals a multiconfigurational character in which the important contribution of doubly excited configurations is especially remarkable for the $2^1A'$ state. Taking the 6a″ orbital as the HOMO (H) and the 7a″ as the LUMO (L) (see Figure 2), three excitations,

TABLE 5: CASSCF and CASPT2 Calculated Excitation Energies (eV) and Oscillator Strengths, and CASSCF Dipole Moments μ (D) and Transition Moment Directions (Relative to Inertial Axis; deg) for *trans*- and *cis*-Urocanic Acid[a]

	excitation energy			μ	
state	CASSCF	CASPT2	osc strength	CASSCF	TM
			trans-Urocanic Acid		
ground state ($1^1A'$)				4.755 (5.080)	
singlet states					
$2^1A'(\pi\pi^*)$	6.14 (5.86)	4.93 (4.73)	0.1203	6.527 (6.945)	3.2
$1^1A''(n_O\pi^*)$	5.53 (5.11)	5.12 (4.88)	0.0005	2.243 (2.422)	
$3^1A'(\pi\pi^*)$	6.74 (6.56)	5.40 (5.09)	0.3427	5.929 (7.482)	31.8
$2^1A''(\pi 3s)$	5.17	5.47	0.0541	6.828	
$4^1A'(\pi\pi^*)$	7.16 (6.98)	6.00 (6.00)	0.3242	5.466 (4.937)	37.0
$5^1A'(\pi\pi^*)$	7.53 (7.31)	6.50 (6.38)	0.0043	4.959 (5.554)	81.4
$3^1A''(n_N\pi^*)$	6.95 (6.80)	6.86 (6.76)	0.0152	2.959 (3.409)	
triplet states					
$1^3A'(\pi\pi^*)$	3.05 (2.87)	3.24 (3.14)		4.531 (4.970	
$2^3A'(\pi\pi^*)$	4.52 (4.31)	4.76 (4.58)		3.186 (3.596)	
$1^3A''(n_O\pi^*)$	5.34 (4.33)	5.01 (4.76)		2.277 (2.910)	
$2^3A''(n_N\pi^*)$	6.34 (5.74)	6.18 (5.94)		3.298 (3.421)	
			cis-Urocanic Acid		
ground state ($1^1A'$)				3.223 (3.351)	
singlet states					
$2^1A'(\pi\pi^*)$	5.47 (5.47)	4.16 (4.15)	0.4568	2.374 (2.368)	−38.6
$3^1A'(\pi\pi^*)$	6.01 (6.01)	5.19 (5.19)	0.0058	1.162 (1.149)	68.8
$1^1A''(n_O\pi^*)$	5.04 (5.04)	5.31 (5.31)	0.0004	5.153 (5.157)	
$2^1A''(n_N\pi^*)$	6.11 (6.11)	5.37 (5.36)	<0.0001	6.506 (6.504)	
$3^1A''(\pi 3s)$	5.31	5.67	0.0303	6.511	
$4^1A'(\pi\pi^*)$	6.61 (6.61)	5.85 (5.85)	0.1382	2.629 (2.260)	16.3
$5^1A'(\pi\pi^*)$	6.89 (6.89)	6.65 (6.65)	0.0709	1.677 (1.677)	80.0
triplet states					
$1^3A'(\pi\pi^*)$	2.29 (2.23)	3.02 (3.03)		2.578 (2.621)	
$2^3A'(\pi\pi^*)$	4.14 (4.15)	4.75 (4.75)		3.231 (3.240)	
$1^3A''(n_O\pi^*)$	4.88 (4.87)	5.14 (5.14)		5.118 (5.123)	
$2^3A''(n_N\pi^*)$	6.14 (6.14)	5.42 (5.41)		6.911 (6.908)	

[a]Values are given for both the CASSCF and MP2 optimized geometries, the latter appearing within parentheses.

H → L, H → L + 1, and H − 1 → L, contrive to be the main contributors to the wave function for these three A′ singlets. The H → L excitation contributes most strongly to the description of the wave function in the $3^1A'$ state, which also has the largest oscillator strength of the computed spectrum.

It is interesting here to compare the structure of this wave function with that of the cis isomer, where the $2^1A'$, $3^1A'$, and $4^1A'$ states have been computed at 4.16 eV (oscillator strength 0.457), 5.19 eV (0.006), and 5.85 eV (0.138). The two low-lying $\pi\pi^*$ excited singlet states of the cis isomer, unlike those of the trans, are mainly described by one single configuration, H → L and H − 1 → L, respectively. The electronic transitions are clearly red-shifted, most markedly in the case of the low-lying transition involving the $2^1A'$ state, and have quite different intensities compared to the corresponding transitions of the trans isomer.

An analysis of the orbital compositions (Figure 2) may serve to help in understanding the structure of the spectra. In the cis isomer, the 6a″ (HOMO) orbital mainly describes the bonding combination of the three double bonds of the molecule, while the 7a″ (LUMO) orbital describes the antibonding combination. The HOMO−LUMO bandgaps are much smaller, at the SCF level, for the cis isomer, leading to a decrease in the excitation energies as compared with the trans isomer. For the cis isomer, one can clearly predict a large change in geometry (also in energy) upon relaxation on the $2^1A'$ $\pi\pi^*$ state, because the excitation (H → L) leads to a weakening of the three double bonds, an effect that will not be so pronounced in the trans isomer. Described mainly by the single excitation H → L, the $2^1A'$ state is responsible for the most intense transition of the computed spectrum of the cis isomer. The considerable contributions of doubly excited configurations to the wave functions of the $3^1A'$ and $4^1A'$ states of the cis isomer, at 23% and 38%, respectively, are worth noting.

The low-lying $n\pi^*$ excitation is computed for the trans isomer to occur at 5.12 eV with an oscillator strength of 0.0005. The CASSCF wave function describes the associated state comprising mainly one singly excited configuration, 30a′ → 7a″. Orbital 30a′ is plotted in Figure 2 and shows a distinctly lone-pair nature, localized on the carbonylic oxygen. The second transition, $n\pi^*$ related to the $2^1A''$ state, is computed at 6.86 eV with a trivially small oscillator strength. The excitation can be described as a one-electron promotion from the σ lone-pair orbital of the ring nitrogen. In the cis isomer, the corresponding transitions have been computed to be nearly degenerate at 5.31 and 5.37 eV, respectively, with small oscillator strengths. The $n\pi^*$ states considered can all be described by a single configuration in their wave functions.

In order to place the beginning of the Rydberg series on these molecules, the first member of the series has been computed in both cases. As has been explained in section 2, the first Rydberg series involve excitations from the highest-lying π occupied orbital. The π → 3s transition has been computed at 5.47 eV (oscillator strength 0.054) and 5.67 eV (0.030), respectively, for the trans and cis isomers. The position of the Rydberg transitions well above the low-lying singlet and triplet $\pi\pi^*$ and $n\pi^*$ excitations, including the most intense transitions, in both isomers guarantees the minor role of the Rydberg states on the main photochemistry of the system and inspire confidence in the accuracy of the calculations.

In summary, the low-lying structure of the vertical absorption spectrum of the trans isomer is formed by one $\pi\pi^*$ transition with medium oscillator strength followed by the lowest $n\pi^*$ excitation involving the oxygen σ lone pair, and finally the most

TABLE 6: CASSCF Wave Functions for *trans*- and *cis*-Urocanic Acid: Principal Configurations,[a] Weights and Number (Weights) of Singly (S), Doubly (D), and Triply (T) Excited Configurations[b] with Coefficients Larger than 0.05

			no. configs (weights)		
state	principal configs	%	S	D	T
		trans-Urocanic Acid			
$1^1A'$	...4a″30a′5a′6a″	88.5		8 (6.7%)	
$2^1A'$	6a″ → 7a′	19.5	9 (67.1%)	8 (24.1%)	
	6a′6a″ → 7a″7a″	11.6			
	6a″ → 8a″	24.8			
	5a″ → 7a″	17.9			
$1^1A''$	30a′ → 7a″	91.8	1 (91.8%)	1 (0.4%)	8 (4.8%)
$3^1A'$	6a″ → 7a″	49.5	7 (82.2%)	11 (6.4%)	1 (0.3%)
	6a″ → 8a″	21.3			
$4^1A'$	6a″ → 7a″		10.1	7 (76.5%)	13 (11.3%)
	6a″ → 8a″	22.7			
	6a″ → 9a″	12.4			
	5a″ → 7a″	23.2			
$5^1A'$	6a″6a″ → 7a″7a″	11.1	7 (52.2%)	23 (37.1%)	1 (0.3%)
	6a″ → 9a″	12.2			
	4a″ → 7a″	31.3			
$3^1A''$	29a′ → 8a″	92.2	1 (92.2%)	2 (0.6%)	2 (4.9%)
$1^3A'$	6a″ → 7a″	50.8	7 (91.0%)	2 (0.8%)	5 (2.2%)
	5a″ → 7a″	31.6			
$2^3A'$	6a″ → 9a″	47.2	8 (86.9%)	7 (3.0%)	5 (2.2%)
	5a″ → 7a″	15.4			
$1^3A''$	30a′ → 7a″	92.0	1 (92.0%)	9 (5.0%)	
$2^3A''$	29a′ → 9a″	92.3	1 (92.3%)	1 (0.3%)	2 (4.5%)
		cis-Urocanic Acid			
$1^1A'$	...30a′4a″5a″6a″	88.6		8 (6.3%)	
$2^1A'$	6a″ → 7a″	67.0	9 (81.3%)	13 (10.4%)	1 (0.3%)
$3^1A'$	5a″ → 7a″	54.1	6 (67.5%)	22 (22.7%)	2 (0.9%)
$1^1A''$	30a′ → 7a″	86.4	1 (86.4%)	4 (4.0%)	7 (3.3%)
$2^1A''$	29a′ → 7a″	91.3	1 (91.3%)	3 (1.5%)	2 (2.1%)
$4^1A'$	6a″ → 7a″	12.9	6 (50.3%)	18 (38.2%)	3 (1.0%)
	6a″6a″ → 7a″7a″	19.8			
	6a″ → 8a″	14.9			
	4a″ → 7a″	17.3			
$5^1A'$	6a″ → 8a″	49.5	8 (81.4%)	8 (6.1%)	3 (1.4%)
	6a″ → 9a″	20.1			
$1^3A'$	6a″ → 7a″	74.7	7 (88.5%)	4 (1.4%)	6 (3.6%)
$2^3A'$	6a″ → 9a″	14.3	14 (88.6%)	4 (1.8%)	7 (3.0%)
	6a″ → 10a″	10.3			
	4a″ → 7a″	51.1			
$1^3A''$	30a′ → 7a″	86.6	1 (86.6%)	5 (3.6%)	5 (2.6%)
$2^3A''$	29a′ → 7a″	92.0	1 (92.0%)	4 (1.2%)	3 (2.2%)

[a] That is, those with weights >10%. [b] With respect to the ground-state principal configuration.

intense transition having a $\pi\pi^*$ character. For the cis isomer, it is the low-lying transition which carries most of the intensity. This is followed by a weak transition and a low-lying and obviously weak $n\pi^*$ excitation, again involving time the oxygen σ lone pair. The Rydberg transitions occur at energies higher than 5.47 and 5.67 eV, respectively, for the two isomers. The structure of the singlet−triplet absorption spectra is similar, with the only difference being that in both isomers the two low-lying excitations are both $\pi\pi^*$ transitions (3.24 and 4.76 eV for the trans isomer and 3.02 and 4.75 eV for the cis). The singlet−triplet gap is considerably larger for the cis isomer. There is, however, one difference between the isomers: in the *trans*-urocanic molecule the two low-lying singlet-triplet excitations are below the first singlet−singlet transitions in the vertical spectrum. In the cis isomer there is only one triplet state below the lowest singlet state.

Figure 3 displays the computed CASSCF transition dipole moment directions for the different transitions in the vertical spectrum. Angles reported in Table 5 are relative to the inertial axes of the respective molecules (long axis shown also in Figure 3).

An analysis of the dipole moments of the different states may help to understand and even to predict the behavior of the related transitions of the spectrum with respect to changes in the environment (although it is worth reiterating that the carboxylic group is deprotonated in aqueous solution). In the trans isomer, all $\pi\pi^*$ transitions relate to states with dipole moments larger than the ground state dipole moment, 4.76 D, all computed at the CASSCF level. The largest difference is on the low-lying $2^1A'$, with a dipole moment of 6.53 eV. In polar solvents, a sizeable decrease in the lowest transition energy may be expected. The situation is reversed in the valence $1^1A''$ and $3^1A''$, which have dipole moments that are considerably smaller, at 2.24 and 2.96 D, respectively. The interaction with polar solvents will obviously lead to corresponding hypochromic shifts in the energies of the $n\pi^*$ transitions. Conversely, in the cis isomer, due to its different molecular structure (ground-state dipole moment 3.22 D) states related to $\pi\pi^*$ excitations have dipole moments smaller than that of the ground state and states related to $n\pi^*$ excitations have larger dipole moments. Except for the $2^3A'$ state on the trans isomer, the situation is reproduced in the triplet states.

3.3. Emission and Nonvertical Absorption Spectra. Experimental studies on the solvated forms of urocanic acid would suggest that the $n\pi^*$ state is lower-lying than the $\pi\pi^*$ first transition. Furthermore, it is proposed that the emission

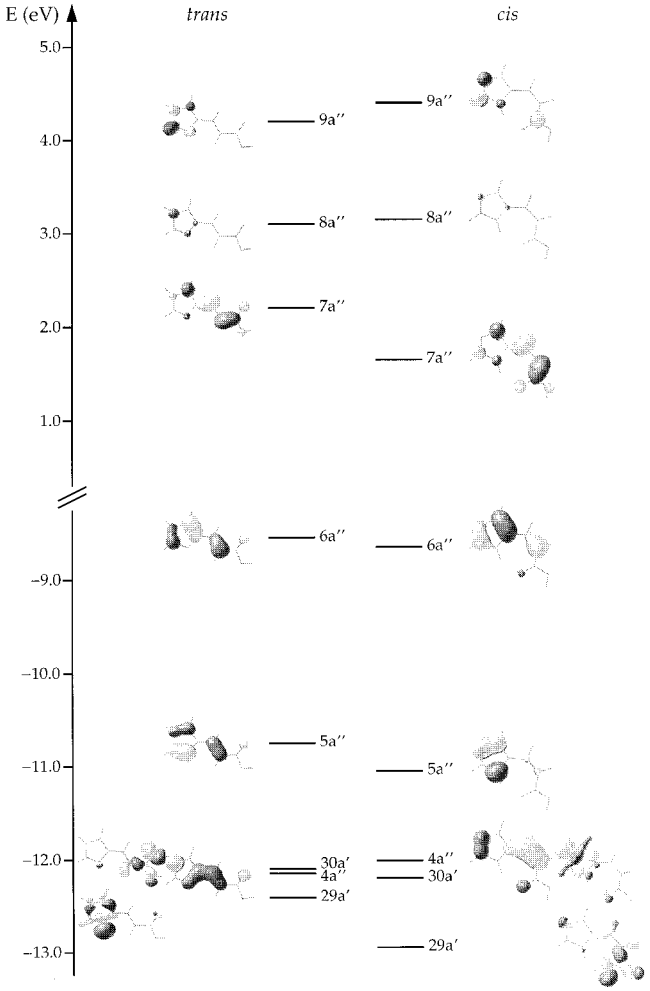

Figure 2. SCF orbital plots for the five highest occupied and three lowest unoccupied MOS of *trans*- and *cis*-urocanic acid.

maximum may be attributed to radiative decay from the nπ* state. To investigate whether these phenomena, which imply a surface crossing between the two states, may be reproduced in the neutral molecule in the gas phase, the band origins and emission maxima have been computed for the lowest $\pi\pi$* and nπ* singlet and triplet states for the two isomers. The band origin, or 0−0 transition, was calculated as the energy difference between the ground state and the given electronic excited state, each at their own respective equilibrium optimized geometries. Emission maxima were calculated as the difference between the excited and ground state energies, both at the excited state equilibrium geometry. These data are compiled in Table 7.

TABLE 7: CASSCF and CASPT2 Calculated Band Origins (0−0 Energies, eV) and Fluorescence/Phosphorescence Maxima (eV) for *trans*- and *cis*-Urocanic Acid

	0−0 energy		E_{max}	
state	CASSCF	CASPT2	CASSCF	CASPT2
	trans-Urocanic Acid			
ground state ($1^1A'$)				
$2^1A'(\pi\pi^*)$	5.52	4.66	4.66	4.17
$1^1A''(n_O\pi^*)$	4.00	4.10	2.25	2.92
$1^3A'(\pi\pi^*)$	2.78	2.54	2.12	2.08
$1^3A''(n_O\pi^*)$	3.98	4.04	2.27	2.90
	cis-Urocanic Acid			
ground state ($1^1A'$)				
$2^1A'(\pi\pi^*)$	4.41	3.37	3.70	3.18
$1^1A''(n_O\pi^*)$	3.69	4.19	2.19	3.26
$1^3A'(\pi\pi^*)$	2.22	2.38	1.63	2.06
$1^3A''(n_O\pi^*)$	3.63	4.12	2.22	3.25

In contrast to the vertical spectrum (Table 5), it can be seen that, in *trans*-urocanic acid, the 0−0 energy for the nπ* transition is quite markedly lower than that obtained for the $\pi\pi$* (a difference of 0.56 eV at the CASPT2 level). The difference between the vertical and 0−0 energies for the nπ* state would suggest that this can be mainly attributed to the topology of the nπ* potential energy surface, with a gradient of almost 1 eV in the differences between the two states. It is therefore proposed that there is a crossing of the nπ* and $\pi\pi$* surfaces close to the ground state geometry.

As should be expected, this sharp decrease in the absorption energy is mirrored in the triplet nπ* transition. However, the lowest lying $\pi\pi$* triplet is so deep that no crossing is observed.

In the cis isomer, no surface crossings are observed between any of the states considered. The differences between the vertical and 0−0 energies in all cases are in the range 0.7−1.0 eV at the CASPT2 level.

4. Summary and Conclusions

The lowest lying states in the gas-phase electronic spectra of *trans*- and *cis*-urocanic acid have been computed theoretically using the CASSCF/CASPT2 method. Because it is not possible to include both static and dynamical correlation in the optimisation procedure, geometries were optimized at both the MP2/6-31G(d) and π-CASSCF/ANO-L(4s3p1d,2s) levels and compared. Serious discrepancies were found between the optimized structures, which have been attributed to the MP2 method overestimating the extent of conjugation within the molecule, an effect that has been noted previously.[25,26]

The important points of the *trans*-urocanic acid spectrum are as follows, with the quoted energies all being at the CASPT2

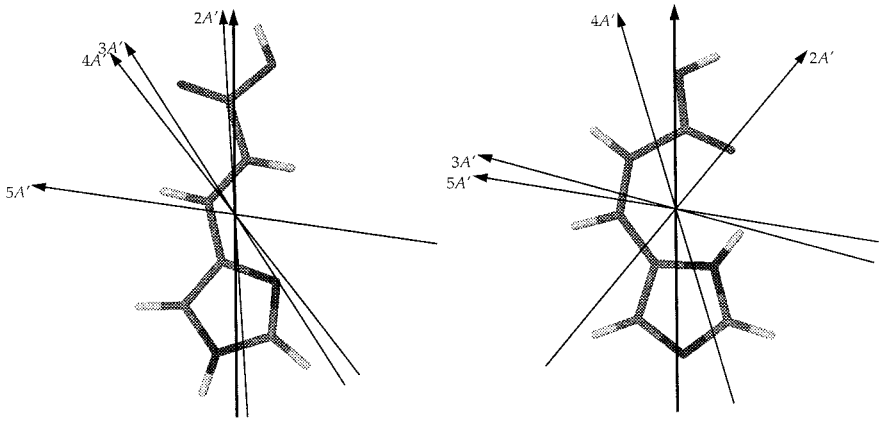

Figure 3. Computed transition moment directions at the CASSI level for the singlet−singlet spectra of *trans*- and *cis*-urocanic acid. The inertial axis is shown in bold.

level. Seven singlet and four triplet vertically excited states were calculated. The spectrum features three intense ($\pi\pi^*$) electronic transitions at 4.93, 5.40, and 6.00 eV, the latter two being the most intense. The lowest lying triplet—also a $\pi\pi^*$ excitation—was calculated at 3.24 eV. The $1^1A''$ $n_O\pi^*$ transition is found to be a weak transition, slightly above the $2^1A'$. However, the computed band origin (0−0 energy) of the $n_O\pi^*$ lies some way below that of the $2^1A'$, implying a surface crossing close to the ground-state geometry. The first Rydberg state (π3s) was calculated to be at 5.47 eV.

In the cis spectrum, seven singlet and four triplet vertically excited states were again computed. The spectrum is dominated by a single ($2^1A'$) $\pi\pi^*$ transition at 4.15 eV, with a second intense band at 5.85 eV. It is noted that the geometry of cis isomer permits the formation of a strong intramolecular N—H···O═C hydrogen bond, which is thought to be the origin of this red shift and other profound differences between the spectra of the two isomers. In particular, the $1^1A''$ $n_O\pi^*$ and $2^1A''$ $n_N\pi^*$ are nearly degenerate at the CASPT2 level. No crossings are observed with the calculation of the 0−0 energies. The first Rydberg state (π3s) was calculated to be at 5.67 eV.

As stated in the Introduction, the authors are preparing a second paper detailing the electronic spectra and photoisomerization pathways of the biologically active, anionic form of urocanic acid. The data presented here, specifically in relation to the near-degeneracy of the $2^1A'$ and $1^1A''$ states in the trans isomer, provide a number of useful insights into the behavior of the deprotonated system. It is hoped that they will further serve to be of use in understanding the gas-phase spectroscopy of this molecule, an experiment that has yet to be performed.

Acknowledgment. The research reported in this paper was performed within the framework of the European Commission TMR network contract ERB FMRX-CT96-0079 (Quantum Chemistry of the Excited State) and the Spanish DGES project PB97-1377. The technical assistance of Wladimiro Díaz and Fernando Durá is most gratefully acknowledged. Massimo Olivucci is also grateful to NATO for grant CRG950748.

References and Notes

(1) Morrison, H.; Deibel, R. M. *Photochem. Photobiol.* **1986**, *43*, 663 and references therein.

(2) Black, H. S.; de Gruijl, F. R.; Forbes, P. D.; Cleaver, J. E.; Ananthaswamy, H. N.; deFabo, E. C.; Ullrich, S. E.; Tyrrell, R. M. *J. Photochem. Photobiol. B: Biol.* **1997**, *40*, 29 and references therein.

(3) Morrison, H. *Photodermatology* **1985**, *2*, 158.

(4) deFabo, E. C.; Noonan, F. P. *J. Expt. Med.* **1983**, *158*, 84.

(5) Reeve, V. E.; Greenoak, G. E.; Canfield, P. J.; Boehm-Wilcox, C.; Gallagher, C. H. *Photochem. Photobiol.* **1989**, *49*, 459.

(6) Noonan, F. P.; deFabo, E. C.; Kripke, M. L. *Photochem. Photobiol.* 1981, 34, 683.

(7) Norval, M.; Gibbs, N. K.; Gilmour, J. *Photochem. Photobiol.* 1995, 62, 209.

(8) Shukla, M. K.; Mishra, P. C. *Spectrochim. Acta* **1995**, *51*, 831.

(9) Hanson, K. M.; Li, B. L.; Simon, J. D. *J. Am. Chem. Soc.* **1997**, *119*, 2715.

(10) Hanson, K. M.; Simon, J. D. *Photochem. Photobiol.* **1998**, *67*, 538.

(11) Ullman, E. F.; Babad, E.; Sung, M. *J. Am. Chem. Soc.* **1969**, *91*, 5792.

(12) Morrison, H.; Bernasconi, C.; Pandey, G. *Photochem. Photobiol.* **1984**, *40*, 549.

(13) Mehler, A. H.; Tabor, H. *J. Biol. Chem.* **1955**, *201*, 755.

(14) Widmark, P.-O.; Malmqvist, P.-Å.; Roos, B. O. *Theor. Chim. Acta* **1990**, *77*, 291.

(15) Andersson, K.; Malmqvist, P.-Å.; Roos, B. O.; Sadlej, A. J.; Wolinski, K. *J. Phys. Chem.* **1990**, *94*, 5483.

(16) Andersson, K.; Malmqvist, P.-Å.; Roos, B. O. *J. Chem. Phys.* **1992**, *96*, 1218.

(17) Roos, B. O. The Complete Active Space Self-Consistent Field Method and its Applications in Electronic Structure Calculations. In *Advances in Chemical Physics; Ab Initio Methods in Quantum Chemistry II*; Lawley, K. P., Ed.; John Wiley & Sons Ltd.: Chichester, England, 1987.

(18) Roos, B. O.; Fülscher, M. P.; Malmqvist, P.-Å.; Merchán, M.; Serrano-Andrés, L. Theoretical Studies of Electronic Spectra of Organic Molecules. In Quantum Mechanical Electronic Structure Calculations with Chemical Accuracy; Langhoff, S. R., Ed.; Kluwer Academic Publishers: Dordrecht, The Netherlands, 1995.

(19) Malmqvist, P.-Å. *Int. J. Quant. Chem.* **1986**, *30*, 479.

(20) Malmqvist, P. Å.; Roos, B. O. *Chem. Phys. Lett.* **1989**, *155*, 189.

(21) Roos, B. O.; Andersson, K.; Fülscher, M. P.; Malmqvist, P.-Å.; Serrano-Andrés, L.; Pierloot, K.; Merchán, M. Multiconfigurational Perturbation Theory: Applications in Electronic Spectroscopy. In Advances in Chemical Physics: New Methods in Computational Quantum Mechanics, Vol. XCIII; Prigogine, I., Rice, S. A., Eds.; John Wiley & Sons: New York, 1996.

(22) Merchán, M.; Serrano-Andrés, L.; Fülscher, M. P.; Roos, B. O. Multiconfigurational Perturbation Theory Applied to Excited States of Organic Compounds. In Recent Advances in Multireference Methods; Hirao, K., Ed.; World Scientific Publishing Co.: Amsterdam, 1998.

(23) Andersson, K.; Blomberg, M. R. A.; Fülscher, M. P.; Karlström, G.; Lindh, R.; Malmqvist, P.-Å.; Neogrády, P.; Olsen, J.; Roos, B. O.; Sadlej, A. J.; Schütz, M.; Seijo, L.; Serrano-Andrés, L.; Siegbahn, P. E. M.; Widmark, P.-O. *MOLCAS* Version 4; Department of Theoretical Chemistry, University of Lund, P.O.B. S-221 00 Lund, Sweden, 1997.

(24) Frisch, M. J.; Trucks, G. W.; H. B. Schlegel Gill, P. M. W.; Johnson, B. G.; Robb, M. A.; Cheeseman, J. R.; Keith, T.; Petersson, G. A.; Montgomery, J. A.; Raghavachari, K.; Al-Laham, M. A.; Zakrzewski, V. G.; Ortiz, J. V.; Foresman, J. B.; Cioslowski, J.; Stefanov, B. B.; Nanayakkara, A.; Challacombe, M.; Peng, C. Y.; Ayala, P. Y.; Chen, W.; Wong, M. W.; Andres, J. L.; Replogle, E. S.; Gomperts, R.; Martin, R. L.; Fox, D. J.; Binkley, J. S.; Defrees, D. J.; Baker, J.; Stewart, J. J. P.; Head-Gordon, M.; Gonzalez, C.; Pople, J. A. *Gaussian 94*, Revision E.2; Gaussian, Inc.: Pittsburgh, PA, 1995.

(25) Bifone, A.; de Groot, H. J. M.; Buda, F. *Chem. Phys. Lett.* **1996**, *248*, 165.

(26) Garavelli, M.; Negri, F.; Olivucci, M. *J. Am. Chem. Soc.* **1999**, *121*, 1023.